Computer model of drying behaviour of ceramic green bodies with particular reference to moisture content dependent properties

Nicolas Lauro, Siham Oummadi, Arnaud Alzina, Benoit Nait-Ali, David Smith

Version of Record: https://www.sciencedirect.com/science/article/pii/S0955221921005124
Manuscript_62079f14079e55943bc7ffcbe37340e2

Computer model of drying behaviour of ceramic green bodies with particular reference to moisture content dependent properties

Nicolas LAURO; Siham OUMMADI;
Arnaud ALZINA; Benoit NAIT-ALI*; David S. SMITH.

July 21, 2021

University of Limoges, IRCER , UMR CNRS 7315, 12 rue Atlantis, F-87068 Limoges, France.

*Corresponding author

Abstract

A numerical model was developed to predict the drying behavior of ceramic green bodies. Resolution of the simultaneous heat and mass transfer equations involved finite elements and the Backward Euler method. Based on experimental data, the model uses equivalent moisture diffusivity, water activity, thermal conductivity and heat capacity as input parameters which depend on moisture content. In particular, the equivalent moisture diffusivity is a key parameter controlling water transport from the body interior to the surface. A simple method was used to estimate the effect of shrinkage on drying rate during the initial drying stage. Predictions of the internal moisture distribution, drying rate and surface temperature as a function of time gave good agreement to experiment for green bodies of alumina paste. External conditions of convection coefficient and relative humidity are shown to sensitively control drying rate and surface temperature evolution during the constant rate period.

Keywords: Drying, Finite element analysis, Alumina, Green bodies

1 Introduction

The fabrication of ceramic products involves several steps: powder selection and preparation, the forming process and the final thermal treatment. Each step is important to obtain a ceramic without defects. In ceramic processing involving a solvent, which is usually water, a drying operation is also needed. If this step is not well mastered, this can lead

to defects such as warping or cracking [1, 2]. Defects can originate from each step in the process and even optimized drying will not solve problems coming from earlier steps such as powder preparation. In all circumstances, due to the initial shrinkage stage, drying should be carefully conducted to remove water from the green body. Drying can be achieved by different techniques but the most commonly used is convective with hot air. This provides the heat required to evaporate water and ensures the removal of the water vapour to far from the body surface. For example, in the ceramic industry, it is well known that the air flow characteristics (temperature, relative humidity, velocity) should be chosen to promote slow drying until shrinkage stops. The energy required to evaporate water is another issue related to drying; in particular for traditional ceramic sectors where large volumes of products are involved. Consequently, methods to optimize the drying stage are of technical importance but also present a strong scientific challenge to understand and control a complex process. In this concern, the work here concerns modeling of the drying behaviour of an initially wet green body.

Drying of ceramics has been studied for many years and the principal physical mechanisms have been identified. Scherer wrote an important review in 1990 with a detailed physical description of these mechanisms [3]. It is well known that drying of a ceramic involves a constant rate period (CRP), where the evaporation rate is constant, followed by one or two falling rate periods (FRP). The shrinkage which occurs at the beginning generally stops during the CRP. More recent work has also contributed to the description of water transfer out of the green body during drying [4, 5]. Another modern approach studies drying through numerical modeling even if creating a mathematical model that takes into account all the mechanisms of such a complex problem is extremely challenging. Finding a satisfactory solution in this case is time consuming and would not necessarily give pertinent returns compared to a simplified model [6]. For this reason, much of the work on modeling uses well chosen simplifications, such as only considering the transfers in one or two dimensions, ignoring shrinkage and variations of thermo-physical properties during drying [7, 8, 9]. This can be seen in the work of Kaya et al. where the convective drying of a product was restricted to a single two dimensional moist surface [9]. On this basis, they managed to predict the appropriate aspect ratio and locations of the air inlet and outlet for optimum heat transfer and drying rate. In their work, Lallemant et al. developed a three dimensional numerical model from the drying profile of a laboratory-scaled ceramic sample [10]. It was then used to predict and optimize the drying process in the case of industrial-scaled products. With similar concerns, Chandra et al chose to predict the transient temperature and moisture distributions in a rectangular moist body subjected to convective drying [11]. In both models, shrinkage and the variation of thermo-physical properties were not taken into account. In another approach, Khalili et al developed a numerical model to calculate stresses induced during shrinkage by measuring experimental strain values of a green clay body. They were able to predict the occurrence of defects, in the form of deformation and/or cracks [12]. Due to the crucial role of water transport in the drying green body, some numerical studies have also been made to evaluate the value of the equivalent diffusion coefficient by identification [13].

The present paper is devoted to the construction and testing of a three dimensional numerical model combining heat and mass transfer to predict the convective drying behaviour of a ceramic green body. No matter how complete the model is, values for the physical properties are always required as input parameters. In fact, the relevant properties such as

equivalent diffusion coefficient for water transport, heat capacity and thermal conductivity vary with the moisture content in the drying body. If numerical models are to be incorporated as an element into process control, prediction accuracy is a key issue. We therefore examine how sensitive the predictions are to the values for the input physical properties. The system chosen for study are ceramic green bodies formed from alumina paste. Alumina is one of the most used and important technical ceramics. Careful experimental measurements were made on the required physical properties of the alumina paste in relation to the moisture content of the drying body. Using this input data, numerical predictions are compared to real results of drying experiments in terms of moisture distribution, drying rate and surface temperature. Compared to previous studies in the literature [7, 8, 9, 10], the novel aspect of the work is the careful attention paid to this input data for obtaining good predictions and assessing how detailed this information needs to be.

Another aspect needing consideration is that the wet ceramic green bodies shrink on drying. The alumina green bodies in this work exhibit essentially isotropic shrinkage, which in a linear direction, does not exceed a value of 5% [14]. This implies that the change in exposed surface area is less than 10% and that the simplification of ignoring dimensional change should not influence accuracy of the calculations too significantly. This was verified in the last section of the paper where surface area reduction due to shrinkage was taken into account by using a simplified method impacting the boundary conditions. Finally the robust nature of the model is demonstrated with a study of the influence of the external conditions on drying behaviour.

2 Mathematical description of the model

Solving a physical problem with the finite element method consists of two major steps: (1) identification of the partial differential equations (PDEs) that describe the behaviours and their boundary conditions; (2) reformulation of the PDEs as a variational problem.

2.1 Definition of the problem

Drying of the ceramic green body by convection involves heat and mass transfers within the system and with the surrounding environment. This situation is illustrated schematically in Fig. 1, where the domain Ω corresponds to the wet body and the boundaries $\partial\Omega$ corresponds to the surface in contact with the air and $\partial\Omega''$ concerns the adiabatic part (no exchange with presence of air) where the fluxes are assumed to be equal to zero.

In order to simplify the problem, the current model is based on the following assumptions:

(1) the wet green body is constituted of an uniform porous solid skeleton and liquid water;

(2) all physical properties for heat and mass transfers are assumed to be isotropic;

(3) even if water migrates through different physical mechanisms (action of capillary pressure, diffusion of water vapour in the porous network), the motion of water in the system is assumed to obey a diffusion law (Fick's law) involving an equivalent diffusion coefficient;

(4) the evaporation of water takes place only at the body surface ($\partial\Omega$) during drying.

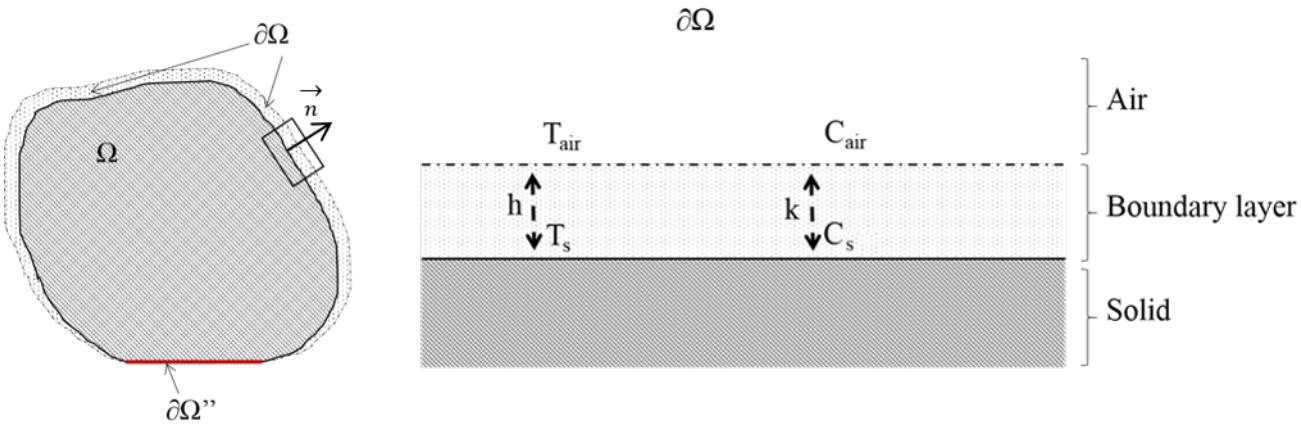

Figure 1: A schematic representation of heat and mass fluxes at a moist surface drying by convection.

The mass transfer inside the body is described by the mass diffusion equation :

$$\frac{\partial C}{\partial t} + \overrightarrow{\nabla} \cdot \overrightarrow{J} = 0 \quad \text{with} \quad \overrightarrow{J} = -D_w \overrightarrow{\nabla} C \tag{1}$$

where C is the water concentration in mol m^{-3} and D_w is the equivalent diffusion coefficient in m^2 s^{-1}. The general heat equation for a homogeneous isotropic medium corresponding to heat transfer in the wet body, is given by :

$$\rho C_p \frac{\partial T}{\partial t} + \overrightarrow{\nabla} \cdot \overrightarrow{Q} = 0 \quad \text{with} \quad \overrightarrow{Q} = -\lambda \overrightarrow{\nabla} T \tag{2}$$

where T is the temperature, λ is the thermal conductivity, ρ is the density, and C_p is the heat capacity.

In the situation of convective drying, only the body surface ($\partial\Omega$) is taken to be directly in contact with the surrounding air. The interaction between the surface exposed to drying and the surrounding air involves a thin film, where the water vapour concentration and the temperature vary, called the boundary layer.

The rate of evaporation at $\partial\Omega$ is proportional to the difference between the water vapour concentration in the air (C_{air}) and the water vapour concentration in the boundary layer at the body surface surface (C_s). The mass flux ($\overrightarrow{J}$) is given by :

$$-\overrightarrow{J} \cdot \overrightarrow{n} = k(C_{air} - C_s) \qquad \text{on} \quad \partial\Omega \tag{3}$$

where $\overrightarrow{n}$ is the outward normal unit vector and k is the mass transfer coefficient in m s^{-1}.

Both concentrations can be related to the water vapour pressure through the ideal-gas law :

$$\begin{cases} C_{air} = RH \frac{P_s(T_{air})}{RT_{air}} \\ C_s = a_w \frac{P_s(T_s)}{RT_s} \end{cases} \tag{4}$$

where RH is the relative humidity, a_w is the water activity, R is the ideal gas constant, and P_s is the saturated pressure of water vapour at T_{air} or T_s, which can be calculated using Antoine's equation [15].

With respect to the heat transfer, heat is supplied through the boundary layer due to the temperature difference between the surrounding air and the body surface. This heat is consumed to evaporate the water at the body surface which tends to establish a state of dynamic equilibrium during drying. The heat flux ($\overrightarrow{Q}$) at the surface is given by :

$$-\overrightarrow{Q}\cdot\overrightarrow{n} = h(T_{air} - T_s) - \overrightarrow{J}\cdot\overrightarrow{n}(L_w M_w) \qquad \text{on} \quad \partial\Omega \tag{5}$$

where h is the heat transfer coefficient, T_{air} is the temperature of air, T_s is the temperature at the body surface, M_w the water molar mass, and L_w is the enthalpy of vaporization for water. The coefficient h depends on whether the convection regime is forced or natural, air velocity and the surface temperature.

Since the mass and heat transfers both occur within the stagnant air film, the mass and heat transfer coefficients are related through the Lewis number k given by the following equation:

$$k = \frac{h}{\rho_a Cp_a Le^{\frac{2}{3}}} \tag{6}$$

where ρ_a is the density of air, Cp_a is the heat capacity of air, and Le is the Lewis number, which can be assumed equal to unity for a water vapour/air mixture [16].

2.2 Variational formulation

The system of equations above represents a strong formulation of the problem (coupling of the heat and mass transfers), which is assumed to be a simultaneously non-linear and time-dependent problem. Turning this PDE problem into a weak formulation goes then through different steps which are summarized as follows :

- Discretization of the time derivative using the backward Euler method in order to obtain a recursive set of stationary relations.
- Multiply the equations of heat and mass transfers by test functions T_{test} and C_{test} which correspond to the mathematical finite element literature.
- Integrate the resulting equations over the domain Ω.
- Perform integration by parts.

Coupling the heat and mass transfers (Eqs. (1) (2) (3) and (5)) yields for a time increment Δt:

$$\begin{aligned}\rho C_p \int_\Omega (T_{n+1} - T_n) T_{test} dx + \int_\Omega (C_{n+1} - C_n) C_{test} dx \; &= -\Delta t\ \lambda \int_\Omega \nabla T_{n+1}\cdot\nabla T_{test} dx \\ &- \Delta t\ D_w \int_\Omega \nabla C_{n+1}\cdot\nabla C_{test} dx \\ &+ \Delta t \int_{\partial\Omega} k(C_{air} - C_{n+1}) C_{test} dS \\ &+ \Delta t \int_{\partial\Omega} h(T_{air} - dt T_{n+1}) \\ &+ L_w M_w k(C_{air} - C_{n+1}) T_{test} dS\end{aligned} \tag{7}$$

Based on Eq. (7) a Python script has been written to calculate the temperature and water distributions as a function of time using the FEniCS open source platform. This platform is devoted to the resolution of partial differential equations with the finite element method as described in [17].

3 Definition of the input parameters

The model presented in this paper requires well determined physical properties in order to give relevant results to compare to experiments. Some of these physical properties are dependent on the moisture content and the distribution of water within the body during drying. The final accuracy of the predictions is sensitive to this aspect. The chosen material for the experiments and the computer modeling was an alumina paste. Wet green bodies were made by casting and contained approximately 30% of water in a dry basis. Further details of the preparation can be found in an earlier paper devoted to shrinkage [14].

3.1 Sample geometry and boundary conditions

The first step in the construction of the model was to create the sample geometry in the form of a mesh using Salome software (version 9.3.0) [18]. Two geometries were studied which correspond to samples used in experimental work. In the first geometry, a square cuboid shape of 15 mm $\times$ 15 mm $\times$ 40 mm was created. This volume was meshed using tetrahedral elements in 3 dimensions as shown in Fig. 2(b) and (c). These dimensions correspond to those used to evaluate the moisture content distribution in a preceding paper [5].

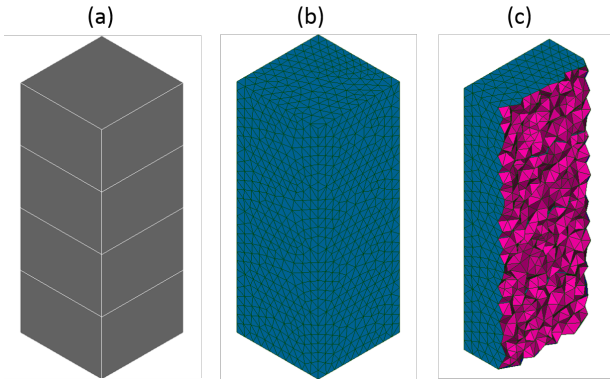

Figure 2: a) Sample geometry, b) sample mesh at the surface, c) sample mesh in the volume.

The boundary conditions used in the model were mathematically described in section 2.1. Fig. 3 illustrates the application of these boundary conditions to the specific sample geometry. The upper surface $\partial\Omega_1$ is in contact with the air, and as such is exposed to convective drying. The sides $\partial\Omega_2$ are considered to exchange heat but without mass transfer since in the experimental work, the lateral surfaces of the samples were covered with a polyvinyl film. Mass transfer can then be assumed to be unidirectional along the length of

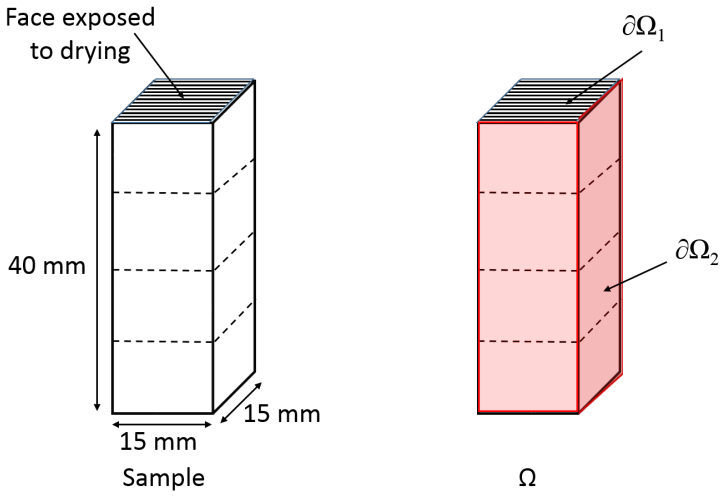

Figure 3: Application of the boundary conditions on the sample.

the sample. The basal surface is considered to be completely insulated (no heat and mass transfers).

In the second studied geometry, a cubic shape with a 20 mm edge was used (Fig. 4) in order to compare numerical predictions in terms of moisture content and surface temperature with experimental data obtained in a climatic chamber. All 5 surfaces, not in contact with the support, were exposed to convective drying. The face in contact with the support is considered to be completely insulated (no heat and mass transfers).

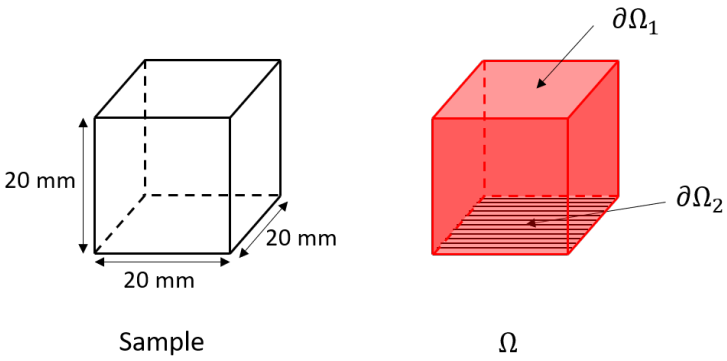

Figure 4: Application of the boundary conditions on the cubic sample.

3.2 Heat transfer convection coefficient

A value of the convection coefficient was determined experimentally in the same environment as the one used for the drying of the samples in this paper. A carbon coated aluminium cylinder was used for this evaluation. The cylinder was heated and then placed inside the climatic chamber with a pyrometer (Lumasense IMPAC IN5 Plus) to measure its surface

temperature. It is assumed that the temperature inside the cylinder is uniform, as its Biot number is less than 0.1. While cooling, the temperature of the surface was measured for 15 minutes. The convection coefficient is determined using the following equation:

$$\frac{T - T_\infty}{T_0 - T_\infty} = e^{-\frac{t}{\tau}} \tag{8}$$

where T is the temperature of the aluminium cylinder, T_0 is the initial temperature of the aluminium cylinder, T_∞ is the temperature of the surrounding air, t is the time in seconds, and:

$$\tau = \frac{\rho\ C\ V}{h\ S} \tag{9}$$

where S is the exchange surface area, V is the sample volume, C is the specific heat capacity of aluminium and ρ is the density of aluminium.

The experimental value for the convection coefficient was determined at approximately 40 W m^{-2} K^{-1} which is the value used in the model. However in 4.2.4 the sensitivity of results to the convection coefficient value was examined.

3.3 Water activity

Water activity (a_w) in a body is a measurable property that depends on temperature and moisture content. It represents the ratio between water vapour pressure at the body surface (P_v) and the saturation pressure above a free water surface (P_s) at the same temperature T:

$$a_w = \frac{P_v}{P_s} \tag{10}$$

There are two distinguishable behaviours for water activity. If the moist surface behaves as a free water surface, which is assumed to be the initial situation with a thin film of water on the surface, then, $P_v = P_s$ meaning that $a_w = 1$. If only bound water remains within the body, held on the internal surfaces, $P_v < P_s$ and then $a_w < 1$.

Experimental measurements of the water activity were made based on the method of equilibrium moisture adsorption of the material at a given temperature. Saturated salt solutions with known activities were used. Thus, the moisture content in the green body was determined at ambient temperature (approx. 20 $°C$) and at 40 $°C$. The wet samples were placed in closed boxes containing the saturated solutions until the mass was stabilized. The weights of the different samples were measured twice: first with the adsorbed water (w_t) and then measured again after complete drying in the oven at 110 $°C$ for 24 hours (w_d). The moisture content on a dry basis (X) of each sample was calculated with the following relation:

$$X = \frac{w_t - w_d}{w_d} \tag{11}$$

Then the experimental points were fitted using the Oswin equation [19] given by :

$$a_w = \frac{1}{1 + (\frac{a}{X})^b} \tag{12}$$

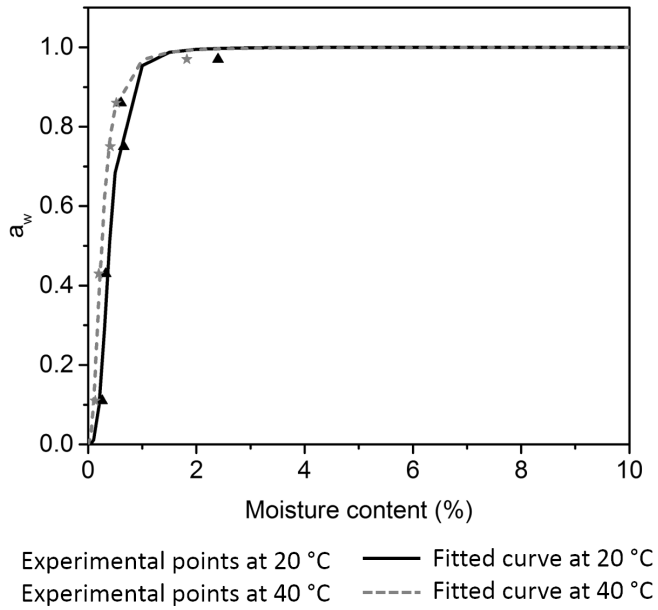

Figure 5: Water activity as a function of moisture content for alumina at ambient temperature (approximately 20 °C) and 40 °C (experimental data and fitted curves).

where a and b are constants.

Based on Fig. 5, examination of the experimental water activity values during drying reveals that the surface behaves as a free water surface until less than 3% moisture content is achieved. As the remaining moisture within the body is extracted, the activity strongly decreases. Furthermore, it should be noted that a small difference between activity values at ambient temperature and $T = 40$ °C occurs for low moisture content.

3.4 Diffusion coefficient

The equivalent moisture diffusion coefficient is a parameter that describes migration of water through the body to be evaporated at the surface. It takes into account the transport of water in liquid and/or in vapour form. For the drying of ceramic materials in an environment with constant conditions, i.e relative humidity and temperature of the drying-air remain stable, several stages can be identified where water behaves differently. During a first period of drying involving shrinkage, the system is assumed to be constituted of solid grains and liquid water which is transported through capillary action. At this stage there is no water vapour diffusion within the body. However, when the body volume is fixed and water evaporates from the pores in the interior of the body, the distribution of water within the sample varies with position. Consequently the process of vapour diffusion becomes limiting and the variation of D_w must be taken into account in the model.

A number of studies have focused on obtaining values for the diffusion coefficient during drying. Some methods are based on numerical modeling, using variation of D_w to fit the calculated water distribution to the one obtained experimentally [20]. Others used purely

experimental results to approximate a value for the diffusion coefficient [21]. Experimental data concerning this second period are published in our recent work where an estimation of the diffusion coefficient as a function of moisture content was made for alumina green bodies [5]. The relationship between D_w and moisture content is of the form:

$$D_w(X) = 2 \times 10^{-9} exp(0.3X) \tag{13}$$

where X is the moisture content on a dry basis. During the first period of drying, no clear water content gradient can be observed within the material with sample dimensions used in the experimental work. This initial period is not taken into account by Eq. (13). A value for the diffusion coefficient during this phase will be determined numerically in the fourth section of this paper.

3.5 Specific heat capacity

In the present study, the modeled material is a paste made of alumina and water which we consider as homogeneous at the macroscopic scale. Its specific heat capacity can thus be estimated with the rule of mixtures.

$$Cp = \frac{X\ Cp_{water} + Cp_{solid}}{X + 1} \tag{14}$$

where Cp_{water} is the specific heat capacity of water (4210 J K^{-1} kg^{-1} at 20 °C), and Cp_{solid} is the specific heat capacity of alumina (760 J K^{-1} kg^{-1} at 20 °C).

3.6 Thermal conductivity

The thermal conductivity of wet alumina green bodies during drying was determined with the transient plane source technique [22]. Experimental measurements show three distinct regimes as a function of moisture content (X). They are fitted by using equations of the form:

$$\lambda = a\ X + b \tag{15}$$

where a and b are constants determined for each regime.

It can be noted that if a sample is only subjected to convective drying, the rate of evaporation should not depend on the thermal conductivity λ in the first period of drying [22]. However when a heat source is added, a heated platform for example, a variation in thermal conductivity should induce a variation in the drying rate of the sample. This is because the conductivity controls a portion of the heat transported to the evaporating boundary layer.

4 Results and discussion

A sensitivity study of the model predictions was first made to understand the impact of material transport parameters. The numerical model was then confronted with two sets of experimental results to validate the accuracy of its results. This allowed the use of the model to predict the effect of external conditions on the constant rate period.

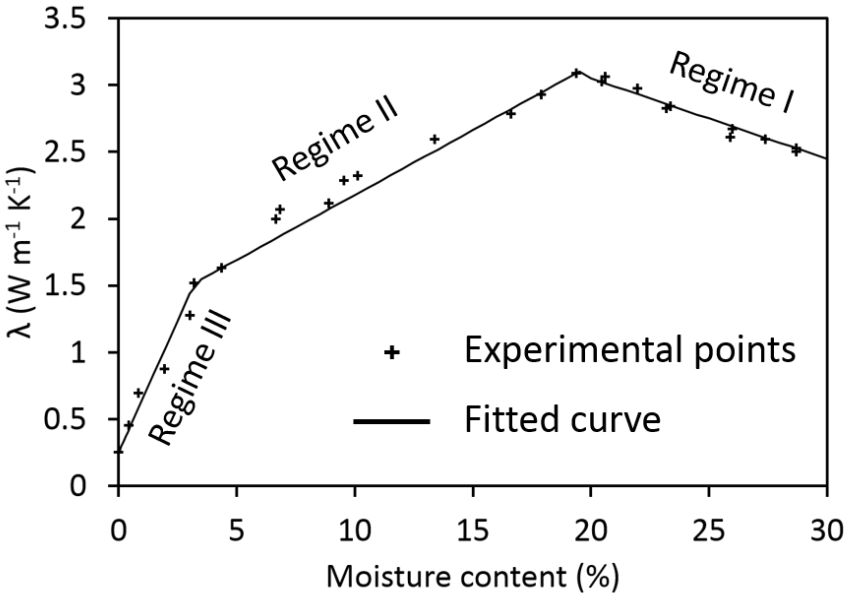

Figure 6: Thermal conductivity as a function of moisture content for a drying green body of alumina (experimental data and fitted curves).

4.1 Sensitivity of model predictions to material transport parameters: equivalent diffusion coefficient and thermal conductivity

From previous experimental work, with similar sample size and drying conditions to those used in the present study, it has been shown that during the major shrinkage stage the water content of the drying sample is uniformly distributed throughout the material at any given time [5]. This means that the internal diffusion of the water is rapid and not limiting for the evaporation rate at the surface of the sample. During this period, the factor limiting the drying rate of the sample is the heat flux entering through its exposed surface determined by the conditions described in Eqs. (3) to (6). In section 3.4, Eq. (13) was introduced to describe the behaviour of the effective diffusion coefficient. While this relation gives an accurate description of the experiments at low moisture content values, a different expression is required to describe the diffusion coefficient D_w during initial drying at high moisture content. In this section, the goal was to identify the value of D_w for which a moisture content gradient starts to appear within the sample.

In order to pinpoint this critical value of D_w, several simulations were run with values for D_w ranging from 1 m^2 s^{-1} to 10^{-8} m^2 s^{-1} for the sample geometry described in Fig. 3.

Fig. 7 shows the surface temperature and local moisture content over time, obtained via simulation, for two different values of diffusion coefficient. For each simulation, the moisture content was plotted at 9 different positions along the length of the sample. The calculated results for values of $D_w > 10^{-6}$ m^2 s^{-1} are not shown as they displayed the same behaviour as Fig. 7(a) : uniform distribution of moisture content throughout the sample for the whole duration of the first period of drying. For $D_w = 10^{-7}$ m^2 s^{-1}, Fig. 7(b) reveals a non uniform moisture content distribution starting immediately at the beginning of the drying

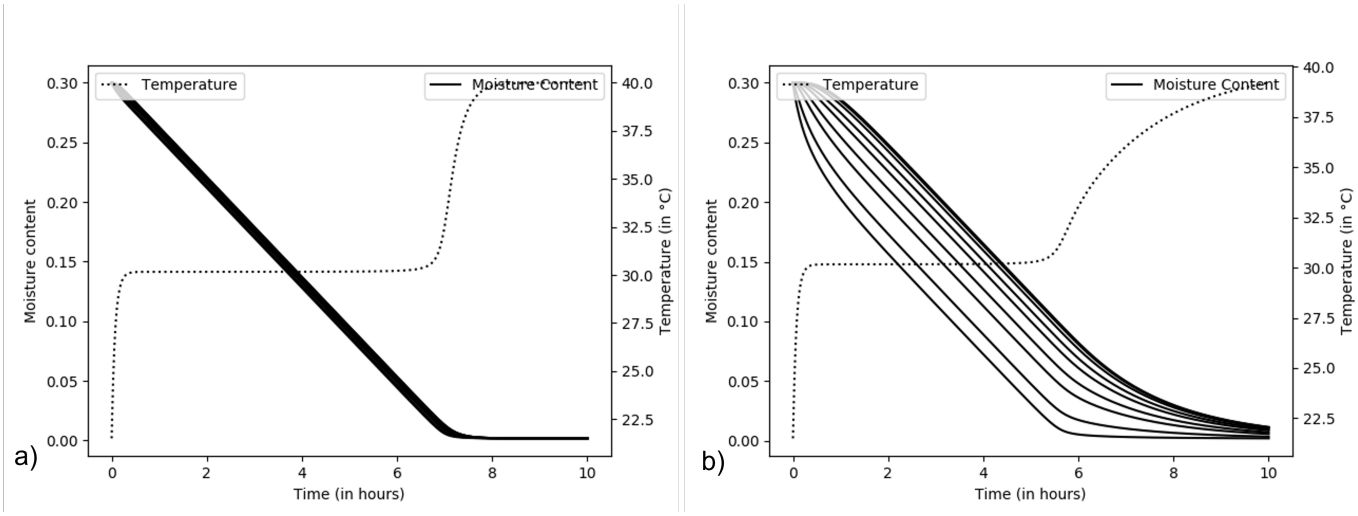

Figure 7: Simulated moisture content versus time at 9 different positions along the drying sample length for a) $D_w = 10^{-6}$ m^2 s^{-1}, and b) $D_w = 10^{-7}$ m^2 s^{-1}, with a drying air at 40 °C and 22.5% RH. The top curve corresponds to the base of the sample. The bottom curve corresponds to the exposed surface.

process. This is different from the actual experimental behaviour of the drying alumina sample, which presents only a very slight moisture content gradient during initial drying. The critical value, below which the sample starts to develop a concentration gradient in moisture, is $D_w = 10^{-6}$ m^2 s^{-1}. As such, for the model presented in this paper, the value of D_w chosen for the first period of drying is $D_w = 10^{-6}$ m^2 s^{-1}, which is well adapted to the size of our samples. When the moisture content $X \leq 19\%$, this value of D_w is replaced by Eq. (13).

The temperature of the surface exposed to drying is also plotted in Fig. 7. After an initial transient response to the imposed drying conditions the temperature stabilizes at a constant value during a period corresponding to the CRP. In both situations presented in Fig. 7, after the CRP, the second rise in temperature is explained by the moisture content at the body surface which has been reduced below 3% (Fig. 5), the value for which the water activity starts to decrease. According to Eqs. (3), (4) and (5), the rate of evaporation decreases and the surface temperature increases.

Experimental studies (Fig. 6) have also shown that the thermal conductivity λ varies with the moisture content of the drying sample. To assess the significance of this parameter, simulations were first made with just a fixed value of thermal conductivity. However due to the absence of a thermal gradient within the body, the thermal conductivity will not have any impact on the surface temperature during drying. That is why, in order to study the thermal conductivity impact on the surface temperature of the sample, simulations were made using the sample geometry depicted in Fig. 4 with an imposed temperature of 25 °C on the bottom face. The simulations were run for a drying air at 30 °C and a relative humidity of 50% with the values: $\lambda = 1.5$ W m^{-1} K^{-1} and $\lambda = 3$ W m^{-1} K^{-1}. These values were chosen to represent the green body thermal conductivity of kaolin paste ($\lambda = 1.5$ W m^{-1} K^{-1}) and alumina paste ($\lambda = 3$ W m^{-1} K^{-1}).

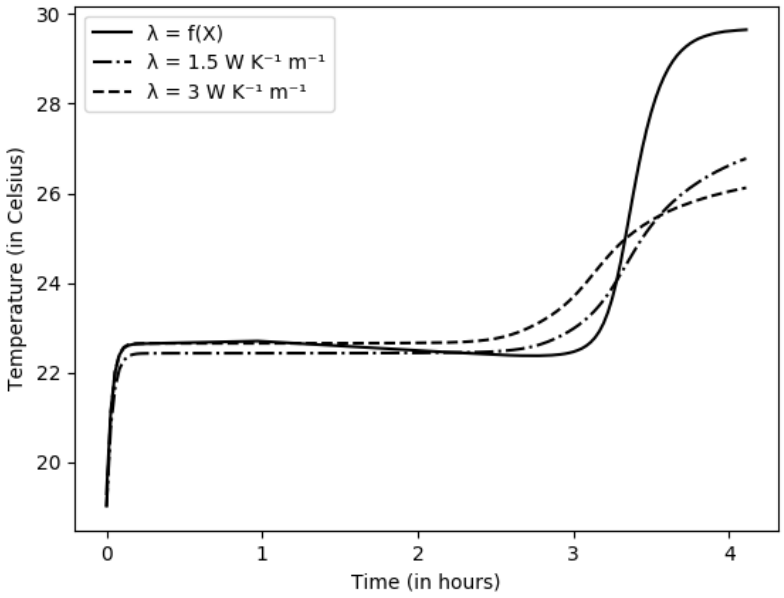

Figure 8: Surface temperature versus time of a drying alumina sample for two fixed values of thermal conductivity. A third uses a conductivity value which varies as a function of moisture content as in Fig. 6, with a drying air at 30 °C and 50% RH. The bottom face is maintained at 25 °C.

The results are shown in Fig. 8 where the surface temperature of the sample is plotted versus time. Two interesting features are revealed. First, the plateau of each curve does not occur at exactly the same temperature. This plateau occurs when the heat coming from the sample and from the surrounding air is equal to the heat required to evaporate the water at the drying surface of the sample. The plateau occurring at a higher temperature for $\lambda = 3$ W m^{-1} K^{-1} is coherent with what could be expected. A higher thermal conductivity implies a higher surface temperature. In turn, the higher surface temperature leads to a higher drying rate as governed by Eqs. (3) and (4). The drying rate during the constant rate period was determined to be 1.06 g h^{-1} for $\lambda = 1.5$ W m^{-1} K^{-1} and 1.12 g h^{-1} for $\lambda = 3$ W m^{-1} K^{-1}.

It is also interesting to note the impact of using a moisture dependent thermal conductivity for alumina instead of a constant value. As revealed by Fig. 8, the first stage of drying (constant rate period) is slightly increased in duration with a plateau temperature which reduces slightly as the conductivity starts to drop significantly at lower moisture contents. After the CRP, the slope of the rise as well as the final temperature value are also strongly affected due to the low thermal conductivity at the end of drying (0.25 W m^{-1} K^{-1} in Fig. 6). It is then preferred to take this physical characteristic into account as precisely as possible for accuracy of the calculations.

4.2 Validation of model

A major step in the process of building a robust numerical model is validating its results in relation to experimental results. It is extremely important to ensure the coherence of the model, geometry and boundary conditions. Two different sample shapes were used, one to investigate the mass transfer, the other to examine both mass transfer and body temperature.

The experimental data obtained in previous work, briefly introduced in terms of geometry and boundary conditions in section 3.1, were compared with predictions using the numerical model. The drying air was fixed at a temperature of 40 °C with a relative humidity of 15%.

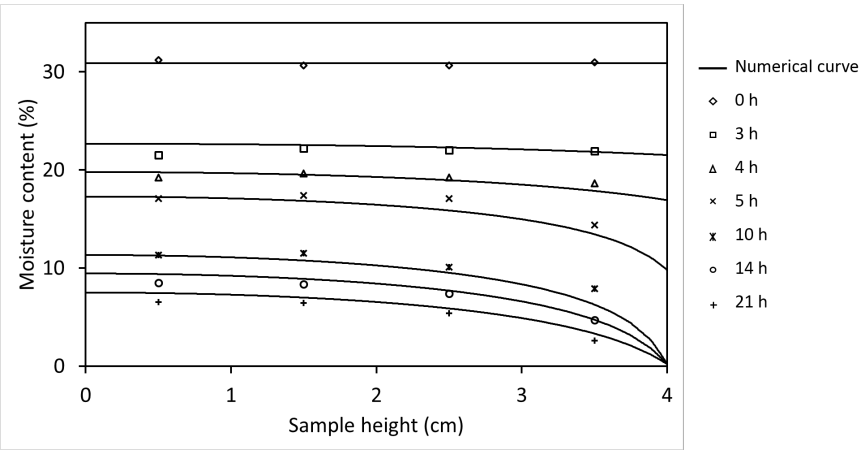

Figure 9: Water distribution in an alumina sample during drying, with a drying air at 40 °C and 15% RH.

Fig. 9 reports results of an experiment which, after selected drying times, quantifies the moisture content of the sample at different positions along its height axis. It was obtained by preparing multiple samples of the same size and drying them simultaneously. At precise times, one of the samples was taken out of the chamber, cut into 4 equal parts and weighed to determine its moisture content. It can be seen that the calculated moisture content after different drying times using the numerical model is in good agreement with experimental results.

The other validation experiments were conducted with a cubic sample of alumina as illustrated in Fig. 4. The sample was placed on a mass balance in a climatic chamber with a drying air temperature fixed at 30 °C and a relative humidity of 45%. All faces except for the one in contact with the balance pan were subjected to convective drying and the loss of mass due to evaporation of water was followed. A pyrometer tracked the surface temperature, which was measured at the center of the upper face.

Fig. 10(a) shows the surface temperature as a function of time for both the experiment and the simulation. The surface temperature calculated through the model fits the experimental temperature. Although a slight difference in surface temperature can be observed, it might be attributed to the boundary condition assigned to the face in contact with the balance pan. The surface of the pan may be heated by the air and exchange some heat through conduction with the sample resulting in a slightly higher temperature throughout drying. Experiments have also shown that the final rise in surface temperature during drying occurs when the

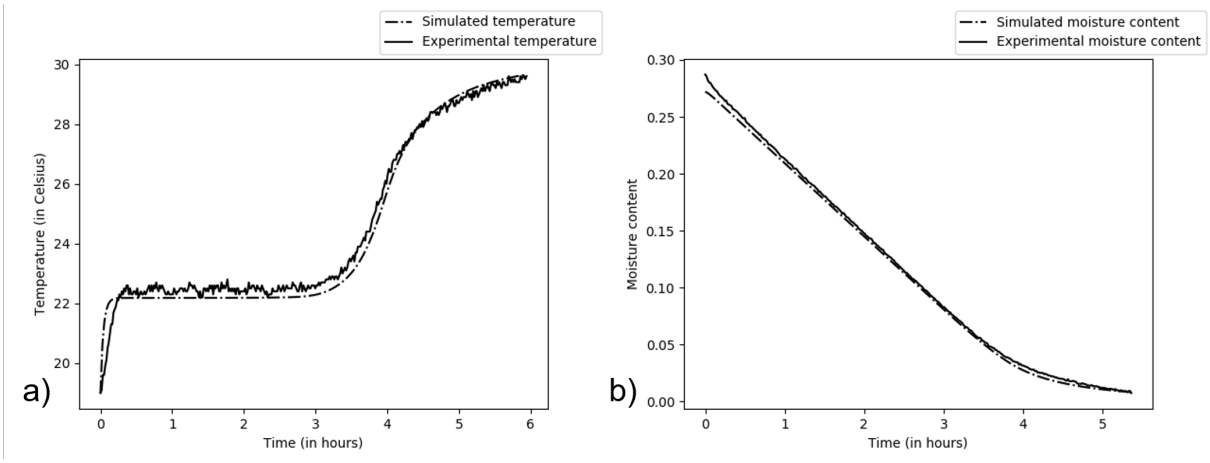

Figure 10: a) Surface temperature and b) moisture content during drying of an alumina sample both experimental and simulated, with a drying air at 30 °C and 45% RH.

drying rate falls off. This phenomenon is shown in Figs. 10(a) and (b) for a drying alumina sample. The decrease in drying rate and the rise in surface temperature are tied together. As the water is evaporated at the surface, the heat exchanged from the surrounding air to the surface tends to form a state of dynamic equilibrium with the heat required to evaporate this moisture. As the constant rate period ends, the drying surface is not saturated in water any more which means that the heat exchanged from the drying air is not contributing uniquely to the evaporation of the water [3]. This leads to a rise in the temperature of the sample, starting from the surface subjected to drying. Measurement of surface temperature can therefore provide a valuable indicator of progress in the drying operation.

The total moisture content of the drying cubic sample has been plotted as a function of time in Fig.10(b) for both the experiment and the simulation. The moisture content predicted by the model is in a reasonable agreement with the measured moisture content. However there is a slight difference in the slopes between the simulation and the experiment; i.e. in the drying rate of the CRP. Several reasons may explain this. One of them is the fact that the model does not take into account the decrease in surface area exposed to drying due to the shrinkage of the sample. A primitive method of taking into account the impact of shrinkage on the heat and mass fluxes at the drying surface was adopted. This involves reducing the heat and mass fluxes proportionally to the calculated surface area due to shrinkage evaluated experimentally. The results, shown on Fig. 11, reveal that the drying rate slows down in the latter stages of the CRP; corresponding to approximately 5% increase in its duration. If accurate quantitative computer model predictions are needed, this aspect should not be neglected in future model development. The drying rate during the CRP is also influenced by external conditions which is examined in the final section of the paper.

4.3 Effect of external conditions on the constant rate period

The external conditions imposed on a drying sample concern the temperature, the convection coefficient and the relative humidity. The last two factors are chosen as variables for study.

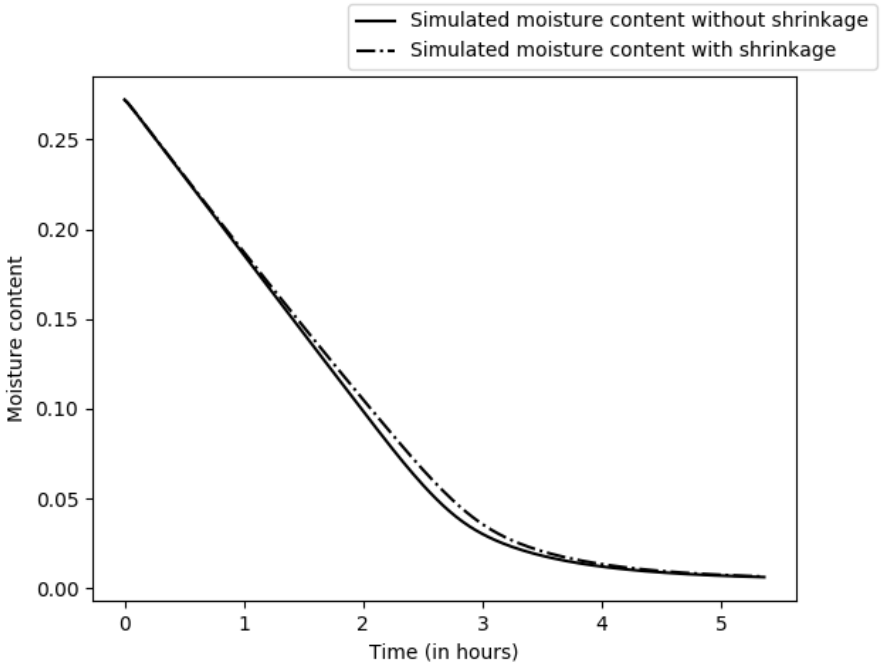

Figure 11: Moisture content and surface temperature of a drying alumina sample subjected to a 30 °C and 50% RH.

The convection coefficient (h) value depends on the drying conditions that the sample is subjected to. The goal was then to observe if a small variation of convection coefficient value would induce significant changes in the drying behaviour of the alumina sample. The values used for the simulations were $h = 35$ W m^{-2} K^{-1}, $h = 40$ W m^{-2} K^{-1}, and $h = 45$ W m^{-2} K^{-1}.

In Fig. 12 it can be seen that the CRP is longest for the lowest value of h. This stage ends when there is not enough water transported to the surface, due to the low diffusion coefficient, eventually leading to decrease in the activity (Fig. 5). The shift of final surface temperature rise with h indicates the sensitivity of drying behaviour to this parameter. A lower value of the convection coefficient means a slower exchange of heat between the surrounding air and the surface of the sample. Conversely higher values of h yield faster drying rates. Increasing h from 35 to 45 W m^{-2} K^{-1} shortens the CRP by approximately 30% which can be easily deduced from Eq. (3) given that heat and mass transfer coefficients are proportional (Eq. (6)).

Drying behaviour is also strongly sensitive to the relative humidity. Fig. 13 shows the moisture content versus time for three different drying air relative humidities. The duration of the CRP is shortened by a factor of 2 with a change of $RH = 75\%$ to $RH = 50\%$, and again from $RH = 50\%$ to $RH = 25\%$. Increase of relative humidity in the drying air is well known as a method to slow the drying rate of ceramic products. Precise knowledge of both h and RH are required for achieving accurate predictions of the computer model.

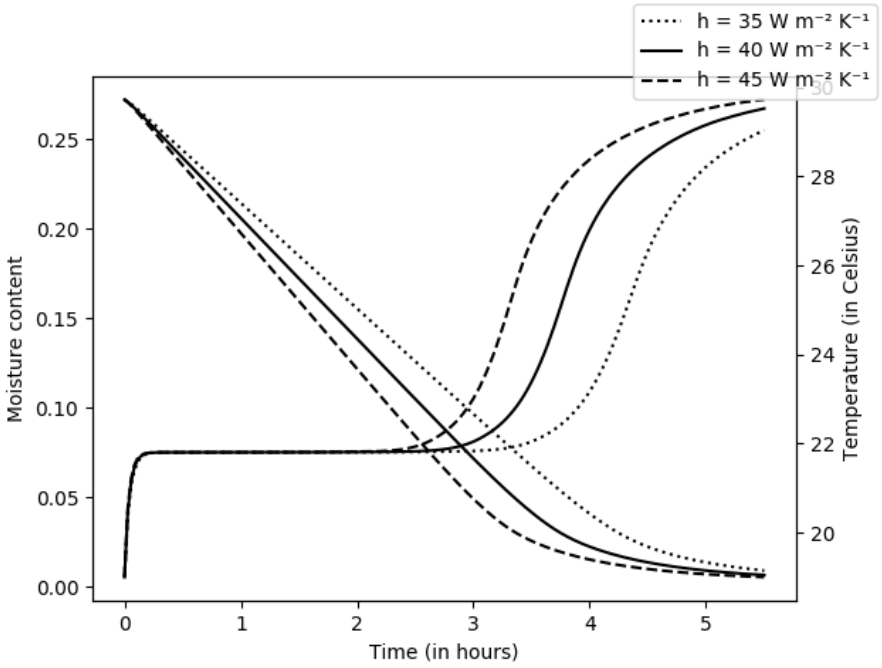

Figure 12: Surface temperature and moisture content during drying for different values of convection coefficient h with a drying air at 30 °C and 50% RH.

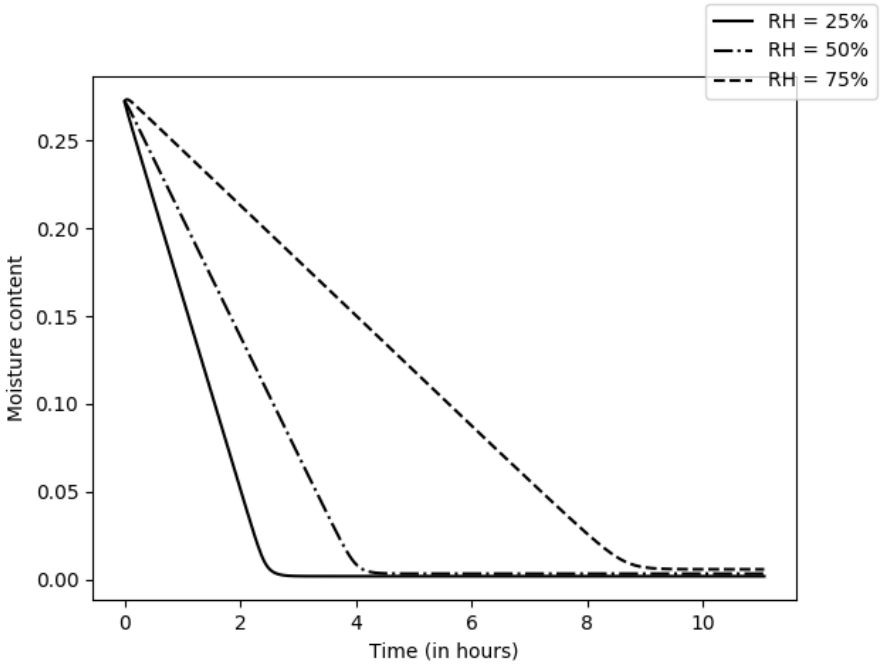

Figure 13: Moisture content during drying for different values of relative humidity RH with a drying air at 30 °C.

5 Conclusion

The ceramic industry seeks to make an increased use of computer models to predict and control drying processes for green bodies. However it is crucial to enter precise values for the thermophysical properties of the system into the model to obtain accurate predictions. In this paper, a three dimensional model combining heat and mass transfer was developed to study the influence of the different thermophysical properties, related to the moisture content of the ceramic green body, on the drying behaviour. It is the examination of this aspect in a detailed manner which is the novel contribution of the work.

Two thermophysical properties are shown to impact significantly the drying kinetics. The equivalent moisture diffusivity and thermal conductivity relate to the material itself and depend on its moisture content. The effective moisture diffusion coefficient, which governs the transport of water (both in liquid and vapour form) inside the body, yields a prediction of the initial drying stage which, for values of $D_w < 10^{-6}$ m^2 s^{-1}, is too short in duration and is associated with a moisture concentration gradient not observed in experiment. Taking into account the dependence of D_w with moisture content is therefore important. The thermal conductivity may also alter the drying kinetics but this only occurs if a second heat source, in addition to heat transfer from convective drying, imposes a thermal gradient in the body. Predictions of drying rate and surface temperature evolution are particularly sensitive to the external conditions surrounding the green body expressed in terms of relative humidity and convection coefficient for the drying air. Accurate computer modeling and optimization of a drying process requires precise values for these parameters. The results confirm the robust nature of the constructed model.

An important takeaway from the work is that the rise in surface temperature of a drying body is intimately linked to the end of the constant rate period. The constant rate period finishes when the drying rate decreases. This happens because less water is transported to the sample surface. Consequently less heat is required for the evaporation of water with the surplus serving to heat the green body, witnessed by the increase of surface temperature. This surface temperature rise is a valuable indicator for the end of the constant rate period.

A factor remains to be examined in greater detail for the drying kinetics: the influence of surface area decrease due to shrinkage. While a preliminary answer has been given in this paper, obtaining a proper answer to this problem will require the use of a model handling the mechanical aspect of large deformation in the body. Furthermore, input data should include realistic elastic properties representing the behaviour of the alumina green body. These steps, foreseen as the topic of a future paper, are necessary for the calculation of internal stresses in the drying ceramic green body.

Acknowledgements

Nicolas Lauro and Siham Oummadi thank the Nouvelle-Aquitaine region for financial support (2019-1R10309). Yassine Bartai is thanked for experimental assistance and Maksoud Oudjedi for valuable discussions.

References

[1] R. Ford. “Ceramics Drying”. In: *Pergamon Press* (1986).

[2] D. Brosnan and G. Robinson. “Introduction to drying of ceramics”. In: *The American Ceramic Society* (2003).

[3] G. W. Scherer. “Theory of Drying”. In: *Journal of the American Ceramic Society* 73.1 (1990), pp. 3–14.

[4] E. Keita et al. “MRI evidence for a receding-front effect in drying porous media”. In: *Physical Review E - Statistical, Nonlinear, and Soft Matter Physics* 87.6 (2013).

[5] S. Oummadi et al. “Distribution of water in ceramic green bodies during drying”. In: *Journal of the European Ceramic Society* 39.10 (2019), pp. 3164–3172.

[6] M.H. Moreira et al. “Direct comparison of multi and single-phase models depicting the drying process of refractory castables”. In: *Open Ceramics* 6 (2021), p. 100111. ISSN: 26665395.

[7] M. Jabbari and J. Hattel. “Modeling coupled heat and mass transfer during drying in tape casting with a simple ceramics–water system”. In: *Drying Technology* 34.2 (2016), pp. 244–253.

[8] A. Kaya, O. Aydin, and I. Dincer. “Heat and mass transfer modeling of recirculating flows during air drying of moist objects for various dryer configurations”. In: *Numerical Heat Transfer; Part A: Applications* 53.1 (2008), pp. 18–34.

[9] A. Kaya, O. Aydin, and I. Dincer. “Numerical modeling of heat and mass transfer during forced convection drying of rectangular moist objects”. In: *International Journal of Heat and Mass Transfer* 49.17-18 (2006), pp. 3094–3103.

[10] L. Lallemant et al. “Modeling of the green body drying step to obtain large size transparent magnesium-aluminate spinel samples”. In: *Journal of the European Ceramic Society* 34.3 (2014), pp. 791–799.

[11] V.P. Chandra Mohan and P. Talukdar. “Three dimensional numerical modeling of simultaneous heat and moisture transfer in a moist object subjected to convective drying”. In: *International Journal of Heat and Mass Transfer* 53.21-22 (2010), pp. 4638–4650.

[12] K. Khalili, M. Bagherian, and S. Khisheh. “Numerical Simulation of Drying Ceramic Using Finite Element and Machine Vision”. In: *Procedia Technology* 12 (2014), pp. 388–393. ISSN: 22120173.

[13] M. Vasić, Ž. Grbavčić, and Z. Radojević. "Determination of the moisture diffusivity coefficient and mathematical modeling of drying". In: *Chemical Engineering and Processing: Process Intensification* 76 (2014), pp. 33–44. ISSN: 02552701.

[14] S. Oummadi et al. "Optical method for evaluation of shrinkage in two dimensions during drying of ceramic green bodies". In: *Open Ceramics* 2 (2020), p. 100016. ISSN: 26665395.

[15] J. Poling, B.; Prausnitz, J. & O'Connell. *The Properties of Gases and Liquids*. 5th Editio. McGRAW-HILL.

[16] F.P. Incropera and D.P. De Witt. *Fundamentals of heat transfer*. 1981.

[17] A. Logg, K. Andre Mardal, and G.N. Wells. "Automated solution of differential equations by the finite element method". In: *Lecture Notes in Computational Science and Engineering* 84 LNCSE (2012), pp. 1–736. ISSN: 14397358.

[18] A. Ribes and C. Caremoli. "Salomé platform component model for numerical simulation". In: *COMPSAC 07: Proceeding of the 31st Annual International Computer Software and Applications Conference*. Washington, DC, USA: IEEE Computer Society, 2007, pp. 553–564.

[19] C. R. Oswin. "The kinetics of package life. III. The isotherm." In: *Journal of the Society of Chemical Industry* 65.12 (1946), pp. 419–421.

[20] U. Telljohann, K. Junge, and E. Specht. "Moisture diffusion coefficients for modeling the first and second drying sections of green bricks". In: *Drying Technology* 26.7 (2008), pp. 855–863.

[21] A.J.J. van der Zanden and M.H. de Wit. "A Procedure to Measure the Diffusion Coefficient of Water in Brick as a Function of the Water Concentration". In: *Drying Technology* 30.5 (2012), pp. 526–534.

[22] B. Nait-Ali et al. "Thermal conductivity of ceramic green bodies during drying". In: *Journal of the European Ceramic Society* 37.4 (2017), pp. 1839–1846.